vertebrate neuromuscular system, we use the Greek prefixes α for those that act on the acetylcholine receptor (by analogy with the well-studied snake toxins), μ for those that act on the muscle membrane sodium channels, and ω for these shaker toxins. In the expectation of characterizing other variants, we designate the peptide described here as ω-conotoxin GVIA.

As with most of the other toxins from *Conus* venoms, the peptide is basic and highly cross-linked by disulfide bridges. In 27 amino acids there are six half-cystines, four positively charged residues, and no acidic groups. Even the α-carboxyl is amidated, which is another feature shared with the other conotoxins. The molecule carries a net charge of 5+.

Perhaps the most striking aspect of the structure is the enormous number of side chains with hydroxyls or other hydrogen-bonding groups. Apart from the six Cys residues that are involved in disulfide bridges, the only amino acid lacking such a function is the solitary Gly. Three residues of hydroxyproline are present; as with the μ-conotoxins (Sato et al., 1983; L. J. Cruz et al., unpublished results) these occur in sequences that differ from those of typical collagen hydroxylation sites.

The physiological studies of Kerr & Yoshikami (1984) indicate that the ω-conotoxin GVIA acts presynaptically, preventing the voltage-activated release of acetylcholine. Release is normally mediated by an influx of calcium, and the evidence is consistent with the toxin's producing an irreversible block of this process. However, much work remains to be done at both the physiological and biochemical level to identify precisely the molecular target of the toxin. The toxin irreversibly blocks the neuromuscular junction, spinal cord, and sympathetic ganglion from frog and the Ca^{2+} component of the action potential in dorsal root ganglion cells in culture from embryonic chick. Clearly, it has some effect on the mammalian central nervous system, but it is without activity on the neuromuscular synapse of mouse. Overall, it appears that the toxin's target is a molecule that is widely present in presynaptic terminals; one exciting possibility is that the toxin irreversibly blocks voltage-activated Ca^{2+} channels.

Acknowledgments

We thank Drs. Doju Yoshikami and Lynne Kerr of the Biology Department, University of Utah, for helpful discussions on their physiological studies and Drs. Howard Morris and Graham Taylor of Imperial College, London, England, for carrying out fast atom bombardment mass spectroscopy.

Registry No. ω-CgTX GVIA, 92078-76-7.

References

Catterall, W. A. (1984) *Science (Washington, D.C.) 223*, 653–661.

Clark, C., Olivera, B. M., & Cruz, L. J. (1981) *Toxicon 19*, 691–699.

Conti-Tronconi, B. M., & Raftery, M. A. (1982) *Annu. Rev. Biochem. 51*, 491–530.

Cruz, L. J., Gray, W. R., & Olivera, B. M. (1978) *Arch. Biochem. Biophys. 190*, 539–548.

Edman, P., & Begg, G. (1967) *Eur. J. Biochem. 1*, 80–91.

Gray, W. R., Luque, A. F., Olivera, B. M., Barrett, J., & Cruz, L. J. (1981) *J. Biol. Chem. 256*, 4734–4740.

Kelly, R. B., Deutsch, J. W., Carlson, S. S., & Wagner, J. A. (1979) *Annu. Rev. Neurosci. 2*, 399–446.

Kerr, L. M., & Yoshikami, D. (1984) *Nature (London) 308*, 282–284.

Mitchell, W. M. (1977) *Methods Enzymol. 17*, 165–170.

Morris, H. R., Panico, M., Barber, M., Bordoli, R. S., Sedgwick, R. D., & Tyler, A. (1981) *Biochem. Biophys. Res. Commun. 101*, 623–631.

Rivier, J. E. (1978) *J. Liq. Chromatogr. 1*, 343–366.

Sato, S., Nakamura, H., Ohizumi, Y., Kobayashi, J., & Yoshimasa, H. (1983) *FEBS Lett. 155*, 277–280.

Stone, B. L., & Gray, W. R. (1982) *Arch. Biochem. Biophys. 216*, 765–767.

Tarr, G. E., Beecher, J. F., Bell, M., & McKean, D. J. (1978) *Anal. Biochem. 84*, 622–627.

Amino-Terminal Arm of the λ Repressor: A ^{1}H NMR Study†

M. A. Weiss, R. T. Sauer,‡ D. J. Patel,§ and M. Karplus*

ABSTRACT: The N-terminal arm of the λ repressor is shown to be flexible in solution by one- and two-dimensional ^{1}H NMR methods. In particular, the relaxation of Thr-2 is largely independent of macromolecular tumbling. The conformation of the operator-binding domain is not affected by the removal of the first three residues nor by a point mutation, Lys-4 → Gln. These results support a proposed model of the λ repressor–operator complex in which the N-terminal arm of the repressor is assumed to be flexible and to wrap around the operator double helix.

The λ repressor consists of two structurally and functionally distinct domains that can be separated by proteolysis (Pabo et al., 1979; Sauer et al., 1979). The N-terminal domain mediates sequence-specific DNA recognition, whereas the C-terminal domain contains strong dimer (and higher order) contacts. The crystal structure of the N-terminal domain, as a fragment of 92 residues, has been determined (Pabo & Lewis, 1982). It consists of five α-helices; the first four fold into a globular structure and the fifth forms a dimer contact. Electron density was not observed for Ser_1-Thr_2-Lys_3, indicating that the first three residues are disordered in the crystal. Fragments lacking these residues bind to operator DNA 100-fold less tightly and give an altered pattern of chemical

† From the Department of Chemistry, Harvard University, Cambridge, Massachusetts 02138. *Received June 13, 1984.* This work was supported by grants from the National Institutes of Health to M.K. (GM-30804) and R.T.S. (AI-16892). M.A.W. is a predoctoral fellow of the Medical Scientist Training Program at Harvard Medical School.

‡ Present address: Department of Biology, Massachusetts Institute of Technology, Cambridge, MA 02139.

§ Present address: Division of Polymer Science, AT&T Bell, Murray Hill, NJ 07974.

0006-2960/84/0423-5090$01.50/0

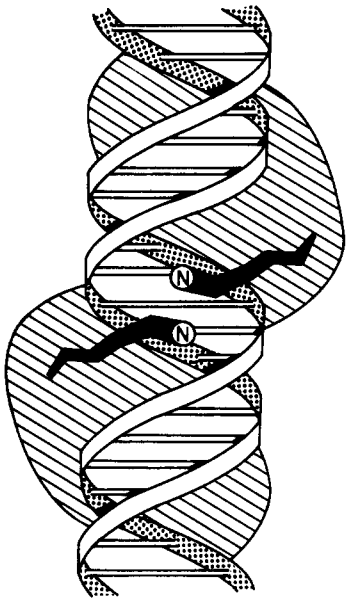

FIGURE 1: Illustration showing proposed role of the N-terminal arm in the repressor–operator complex. As the rest of the protein binds to the "front" of the operator, the arm reaches around to make contacts in the major groove on the "back" of the operator site (shown as the *front* of the illustration).

protection on one face, but not on the other face, of the operator binding site. This suggested that the N-terminal residues of the domain form a flexible, extended "arm" that wraps around the double helix to contact the back of the operator site, as shown in Figure 1. Although the number of residues in the arm is uncertain, in the crystal the first six amino acids (Ser-Thr-Lys-Lys-Lys-Pro) make no obvious contacts with the rest of the domain (Pabo et al., 1982).

To provide more detailed information on the properties of the arm and its role in operator binding, we have undertaken a solution ^{1}H NMR study. Since the model of the repressor–operator complex requires that the arm be flexible (a rigid arm would result in large kinetic barriers to binding and release), we have measured the line widths of specific resonances assigned to the arm. These measurements determine whether the arm moves independently of the rest of the domain (Jardetzky et al., 1978; Buck et al., 1978; Wade-Jardetzky et al., 1979). In addition, using the chemical shifts of assigned aromatic residues as structural markers, we demonstrate that the conformation of the N-terminal domain is not affected by the removal of the first three residues nor by a point mutation at residue 4 (Nelson et al., 1983; Hecht et al., 1983). This mutant protein, in which Lys-4 is replaced by Gln, is shown also to have a flexible arm in solution.

Materials and Methods

The wild-type repressor, the Lys-4 → Gln mutant repressor, and their proteolytic fragments were purified as described (Pabo et al., 1979; Sauer et al., 1979; Nelson et al., 1983; Hecht et al., 1983). The 4–92 fragment was a gift of C. O. Pabo. The 1–102 fragment was encoded by a plasmid constructed by H. Nelson and M. Reach that contained a deletion of the C-terminal portion of the *c*I gene. The 1–102 fragment was purified from overproducing strains of *Escherichia coli* by standard methods, including column chromatography with Affi-Gel Blue, Bio-Rex 70, and Sephadex G-75 resins.

For ^{1}H NMR study, the intact repressors were exhaustively dialyzed against 200 mM ammonium bicarbonate, lyophilized, dissolved in D_2O, lyophilized, dissolved in 340 μL of NMR buffer (see below), and lyophilized. This powder was dissolved

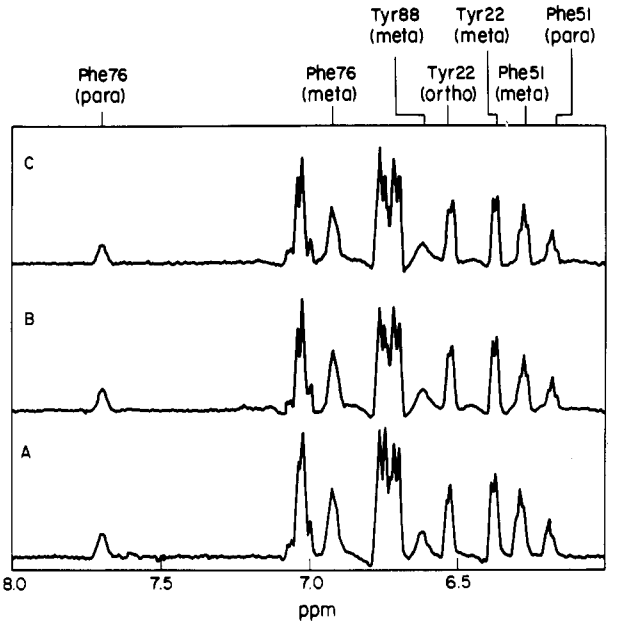

FIGURE 2: Aromatic region of the 500-MHz ^{1}H NMR spectra comparing (A) the wild-type 1–92 fragment, (B) the wild-type 4–92 fragment, and (C) the mutant 1–92 fragment in which Lys-4 is replaced by Gln. Although the global structures of these fragments are essentially identical, the wild-type 1–92 fragment binds operator at least 100-fold more strongly. The assignments shown are described elsewhere (M. A. Weiss, R. T. Sauer, D. J. Patel, and M. Karplus, unpublished results). Spectrum A is the sum of 17 208 scans; spectrum B, of 20 640 scans; and spectrum C, of 27 324 scans. The protein concentration was 0.25 mM, assuming an extinction coefficient of 0.54 cm^{-1} at 280 nm. The recycle delay was 1 s, and resolution was enhanced by convolution difference with parameters GM2, EM15, 0.9.

in 340 μL of 99.96% D_2O, spun for 1 min in a microcentrifuge, and loaded into an NMR tube. The repressor fragments were exhaustively dialyzed against distilled, deionized water and lyophilized. The powder was dissolved in D_2O, lyophilized, dissolved in 170 μL of NMR buffer, spun for 1 min in a microcentrifuge, and loaded into a microcell NMR tube. NMR buffer consists of 200 mM KCl, 50 mM potassium phosphate (pD 7.4, direct meter reading), 1 mM sodium azide, and 0.1 mM ethylenediaminetetraacetic acid.

All spectra were taken at 500 MHz and 30 °C with simultaneous quadrature phase detection. One-dimensional free induction decays were acquired following a 70° pulse with a recycle delay of 1 s. A convolution difference was applied before Fourier transformation as described in the legends to Figures 2 and 4. Two-dimensional correlated spectra were obtained by the method of States and co-workers (Aue et al., 1976; States et al., 1982), as described in the legend to Figure 5.

Results

The aromatic region of the ^{1}H NMR spectrum of the wild-type 1–92 fragment is shown in panel A of Figure 2. The large dispersion of chemical shifts is a result of its structure. In the primary sequence there are six aromatic groups; they are Tyr-22, Phe-51, Tyr-60, Phe-76, Tyr-85, and Tyr-88 (Sauer & Anderegg, 1978). As shown in Figure 3, Tyr-22, Phe-51, and Phe-76 are buried in the hydrophobic interior of the N-terminal domain. Tyr-22 projects from helix 1 to form a hydrogen bond near the N-terminus of helix 2. Phe-51 projects from helix 3 to stack against Tyr-22 near the center of the domain. Phe-76 projects from the turn between helix 4 and helix 5 and is separated from Phe-51 by several buried leucines. Thus, these three aromatic groups relate to all the

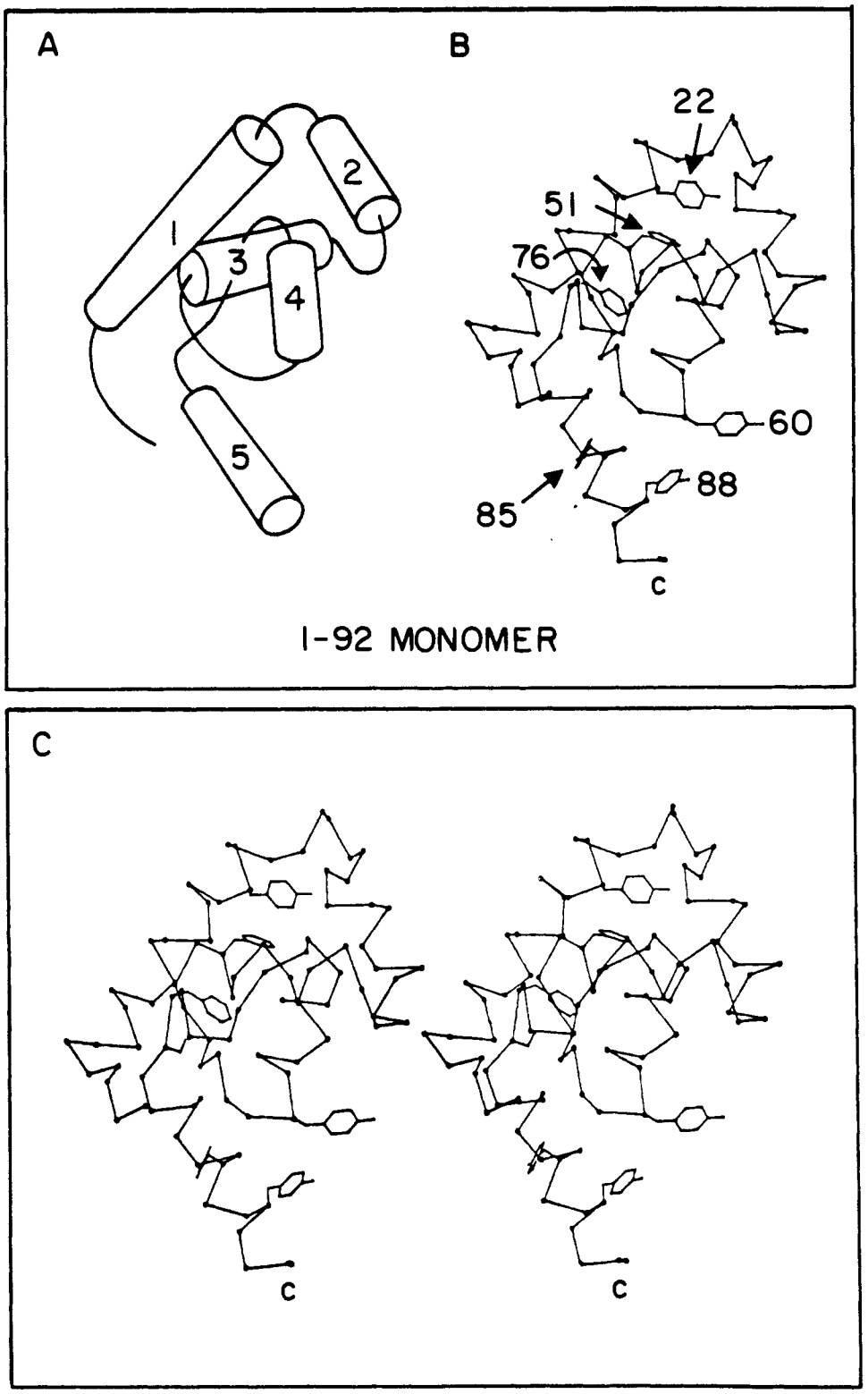

FIGURE 3: (A) Cylinder model and α-carbon representation of the 1–92 domain showing the aromatic side chains. Tyr-22, Phe-51, and Phe-76 are buried in the hydrophobic interior and provide sensitive markers for tertiary structure. (B) Stereopair. The structures shown are calculated from the crystal coordinates of Pabo & Lewis (1982).

helices and, because of their unusual local magnetic environments, provide sensitive markers for tertiary structure. In fact, ring current shift calculations suggest that their resonances should be sensitive to displacements as small as 0.2 Å (Perkins & Dwek, 1980; Hoch et al., 1982); it has been shown that the surface amino acid substitution Gln-44 → Tyr causes small, selective shifts in Tyr-22 and Phe-51 (Weiss et al., 1983). The remaining three tyrosines (residues 60, 85, and 88) are on the surface of the monomer and will not be considered here. Panel B of Figure 2 shows the aromatic spectrum of a 4–92 fragment, which lacks Ser_1-Thr_2-Lys_3. The operator affinity of this fragment is reduced some 100-fold, and yet its aromatic resonances are seen to be virtually identical with those of the 1–92 fragment. This indicates that the folding of the domain is not affected by the removal of the three N-terminal residues. Its reduced affinity and altered pattern of chemical protection on the back of the operator site (Pabo et al., 1982) thus result from loss of local interactions rather than from changes in

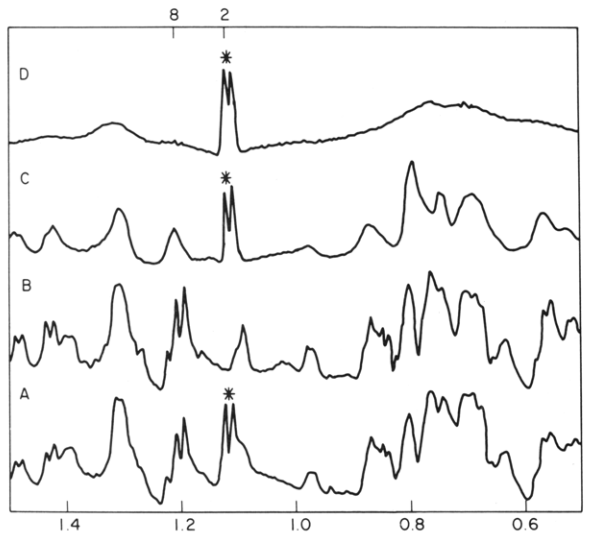

FIGURE 4: Part of the aliphatic region of the 500-MHz ^{1}H NMR spectra comparing (A) the wild-type 1–92 fragment, (B) the 4–92 fragment, (C) the 1–102 dimer, and (D) the intact repressor oligomer. The transverse relaxation (T_2) of Thr-2 is nearly independent of overall rotational correlation time. Spectra A and B are described in the legend to Figure 2. Spectrum C is the sum of 364 transients. The 1–102 concentration was 4.5 mM, assuming an extinction coefficient of 0.675 cm^{-1} at 280 nm. Resolution enhancement is the same as in spectra A and B. Spectrum D is the sum of 1000 transients. The intact repressor concentration was 3 mM, assuming an extinction coefficient of 1.12 cm^{-1} at 280 nm. A convolution difference with parameters GM1, EM4, 0.95 was applied. Thus, spectrum D is more resolution enhanced than spectra A–C. The asterisks in panels A, C, and D indicate the methyl resonance of Thr-2.

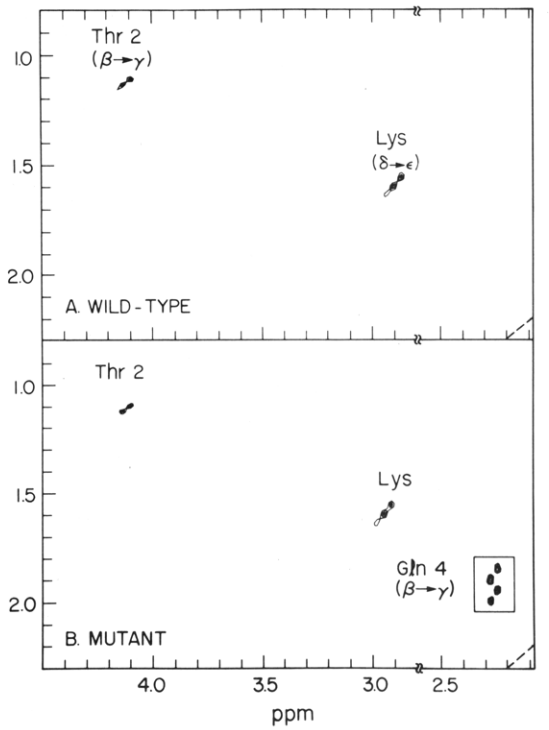

FIGURE 5: Portion of the two-dimensional correlated spectra of (A) the wild-type intact repressor and (B) a mutant intact repressor in which Lys-4 is replaced by Gln. This pulse sequence acts as a dynamic filter, enabling the selective observation of flexible regions of macromolecules. Here the wild-type and mutant arms are seen to be flexible in solution. In spectrum A 64 scans were acquired per t_1 value, and 292 t_1 values were observed. In spectrum B 96 scans were acquired per t_1 value, and 280 t_1 values were observed. The contour levels of Gln-4 (box) extend 3-fold lower than the rest of the spectrum. In both spectra 1024 points were sampled over a sweep width of 5000 Hz in t_2. The t_1 dimension was zero filled to 1024 to create a square data matrix. A convolution difference with parameters GM2, EM20, 1 was applied in both dimensions. Following Fourier transformation, the data matrix was made symmetric by minimum value. The protein concentration was 3 mM. The diagonal peaks are not shown, but their position is indicated by a dashed line in the lower right corner.

global structure. This conclusion is strengthened through the study of a genetically altered domain in which Lys-4 is replaced by Gln. Its aromatic spectrum, shown in panel C of Figure 2, is essentially the same as that of the wild-type domain, implying a correspondence of tertiary structure. Nevertheless, this amino acid substitution reduces operator affinity at least 100-fold (Nelson et al., 1983; Hecht et al., 1983).

The N-terminal domain contains two threonines, located at positions 2 and 8 (Sauer & Anderegg, 1978). Although there is no electron density for Thr-2 in the crystal, Thr-8 is well-defined and interacts with neighboring amino acids (Pabo & Lewis, 1982). Panel A of Figure 4 shows part of the aliphatic region of the ^{1}H NMR spectrum of the wild-type 1–92 fragment. This region includes the methyl groups of alanine, threonine, and the branched-chain aliphatic amino acids (Bundi & Wüthrich, 1979). Two sharp methyl doublets are observed at 1.1 and 1.2 ppm. Two-dimensional correlated experiments demonstrate that these methyl groups belong to AMX spin systems characteristic of threonine (Bundi & Wuthrich, 1979; Wüthrich et al., 1982). They may be assigned by comparison of panel A (1–92) and panel B (4–92). Since the aliphatic spectrum of the 4–92 fragment lacks the doublet at 1.1 ppm, the doublet at 1.2 ppm is assigned to Thr-8 and the doublet at 1.1 ppm to Thr-2.

Panel C of Figure 4 shows the aliphatic spectrum of a dimeric 1–102 fragment. Since this species is about twice the size of the monomeric 1–92 fragment, and therefore has a longer correlation time, its resonances are expected to be broader. Examination of the spectrum shows that this is generally the case. The methyl doublet of Thr-2, however, remains sharp. Panel D of Figure 4 shows the aliphatic spectrum of intact λ repressor, which forms large oligomers at millimolar concentrations. A sharp doublet at 1.1 ppm is observed in this resolution-enhanced spectrum amidst an envelope of broad resonances. In the intact repressor, as in the N-terminal fragment, this doublet has been assigned to Thr-2 through the study of mutants containing successive N-terminal deletions (Weiss et al., 1984). These results demonstrate that the line width (T_2 relaxation) of Thr-2 is largely independent of macromolecular tumbling, which dominates the relaxation of protons in stably folded structures (Jardetzky et al., 1978; Buck et al., 1978; Wade-Jardetzky et al., 1979). Thus, Thr-2 and presumably other N-terminal residues are reorienting independently of overall rotation, indicating that the arm is flexible in solution.

As further evidence for the flexibility of the N-terminal arm, we also present results of a two-dimensional ^{1}H NMR study of the intact protein. As discussed in detail elsewhere (Weiss et al., 1984), two-dimensional correlated experiments are a sensitive probe for flexible regions of macromolecules. The sensitivity of these experiments arises because the amplitude of cross peaks decays rapidly as the line widths approach the coupling constant involved (Piantine et al., 1982; Rance et al., 1983). Line widths of this magnitude occur in stably folded regions of proteins. For the intact λ repressor the effect of such filtering is dramatic. Its correlated spectrum contains only a small number of cross peaks rather than the many hundreds that in principle could occur. Most of these have been assigned to the N-terminal arm (Weiss et al., 1984). Panel A of Figure 5 shows a portion of the correlated spectrum. In the region shown, only two cross peaks are observed; they are the α–β coherence of Thr-2 and the δ–ϵ coherence of

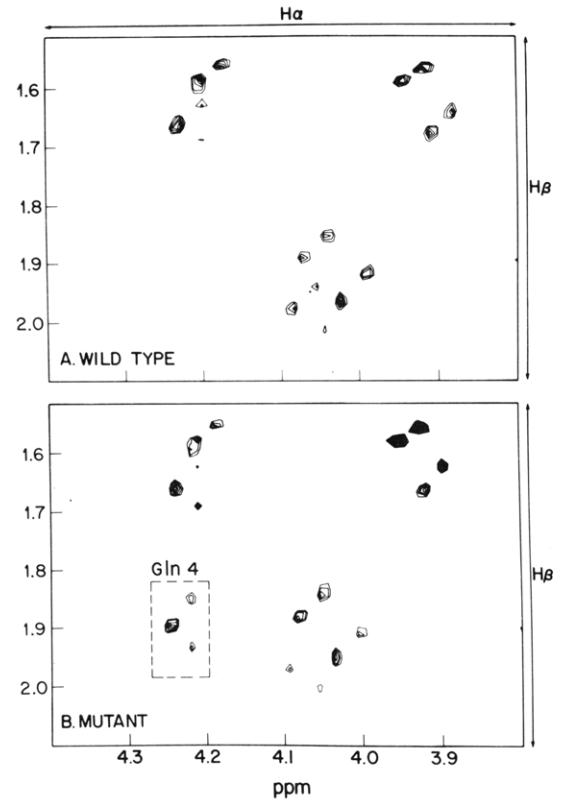

FIGURE 6: Portion of the two-dimensional correlated spectra of (A) the wild-type 1–90 domain and (B) the Lys-4 → Gln mutant 1–90 domain. This region, which contains α–β coherences, identifies the Gln-4 (α–β) cross peak. Additional cross peaks are observed at identical positions at lower contours in both spectra. In spectrum A 48 scans were acquired per t_1 value, and 382 t_1 values were observed. In spectrum B 32 scans were acquired per t_1 value, and 475 t_1 values were observed. The protein concentration was 3 mM. The two-dimensional data were processed as described in the legend to Figure 5.

several lysines. Panel B of Figure 5 shows the corresponding portion of the spectrum of the Lys-4 → Gln mutant repressor. The Thr-2 and lysine signals demonstrate that the arm in the mutant is flexible. In addition, a new cross peak is observed whose position is appropriate for a glutamine β–γ coherence (Bundi & Wüthrich, 1979; Wüthrich et al., 1982); presumably, this is Gln-4. Since the connected α–β cross peak is weak (it does not appear at the contour levels shown), we confirm this assignment by comparing the wild-type and mutant N-terminal fragments. These domains tumble rapidly in solution, so that phase cancellation is not significant and their correlated spectra contain hundreds of cross peaks. Figure 6 shows a region of their two-dimensional spectra containing α–β coherences. The wild-type spectrum is in panel A and the mutant spectrum in panel B. The latter contains an additional cross peak at the same position as the weak signal above. The connected β–γ signal is also observed. We assign this new spin system in the fragment spectrum to Gln-4. By analogy, this assignment extends to the spectrum of the intact mutant repressor and confirms the flexibility of the arm in the mutant.

Discussion

The dynamics of proteins play an important role in ligand binding, catalysis, and macromolecular interactions (Karplus & McCammon, 1983). The motion of structured elements is often emphasized, but order–disorder transitions also represent an important feature (Huber & Bennett, 1983). As an example, flexible loops in the capsid protein of tobacco mosaic virus become ordered in the intact virus, where they interact with the RNA genome (Klug, 1979). Flexibility in this and spherical viruses such as tomato bushy stunt virus (Harrison et al., 1978; Harrison, 1980) may facilitate their assembly. In the current model of the λ operator–repressor complex, the N-terminal arms wrap around the double helix to contact the back of the operator site. Flexibility is an essential feature of this model, since otherwise there would be large kinetic barriers to operator binding and release. The experiments reported here demonstrate that the N-terminal arm is indeed flexible in solution. In addition, they serve as structural controls for the interpretation of biochemical studies of a 4–92 fragment (Pabo et al., 1982). The reduction in operator affinity exhibited by this fragment must reflect the local function of the arm, since the global structure of the fragment is identical with that of the 1–92 fragment. Its altered pattern of chemical protection can thus be used to position these residues against the operator site.

The substitution of Gln for Lys at position 4 reduces operator affinity at least 100-fold (Nelson et al., 1983; Hecht et al., 1983). We have shown that the mutant arm is flexible in solution and the conformation of the domain is unaffected. This implies that the reduced operator affinity results from loss of favorable interactions rather than misfolding. The Lys → Gln substitution removes a potential ionic interaction to the phosphate backbone of the operator. Whether this substitution also affects the folding of the arm (as a whole) against the DNA has yet to be determined.

Conclusions

The N-terminal arm of the λ repressor has been shown to be flexible in solution by ^{1}H NMR. This follows from the demonstration that the line width of Thr-2 in the arm is largely independent of macromolecular tumbling. The conformation of the operator-binding domain is not perturbed by the removal of the first three residues of the arm nor by the point mutation, Lys-4 → Gln. The mutant arm is also flexible in solution, suggesting that its reduced operator affinity results from loss of favorable interactions rather than misfolding.

Acknowledgments

We thank Carl Pabo for his gift of the 4–92 fragment, Carl Pabo and Mitch Lewis for crystal coordinates and discussion, Egon Amaan for wild-type plasmids, and Michael Hecht, Hillary Nelson, and Kathy Hehir for mutant plasmids and advice. The two-dimensional acquisition and processing software was written by David States. Ring-current shifts were calculated with the assistance of Jeff Hoch. We thank Ron Haberkorn, David Ruben, Ed Olejniczak, and Alfred Redfield for advice regarding NMR technique. All spectra were taken at the 500-MHz facility of the Francis Bitter National Magnet Laboratory, supported by NSF Contract G67C.

References

Aue, W. P., Bartholdi, E., & Ernst, R. R. (1976) *J. Chem. Phys. 64*, 2229–2246.

Buck, F., Ruterjans, H., & Beyreuther, K. (1978) *FEBS Lett. 96*, 335–338.

Bundi, A., & Wüthrich, K. (1979) *Biopolymers 18*, 285–297.

Harrison, S. C. (1980) *Biophys. J. 32*, 139–151.

Harrison, S. C., Olson, A., Schutt, C. E., Winkler, F. K., & Bricogne, G. (1978) *Nature (London) 276*, 368–373.

Hecht, M. H., Nelson, H. C. M., & Sauer, R. T. (1983) *Proc. Natl. Acad. Sci. U.S.A. 80*, 2676–2680.

Hoch, J. C., Dobson, C. M., & Karplus, M. (1982) *Biochemistry 21*, 1118–1125.

Huber, R., & Bennett, W. S. (1983) *Biopolymers 22*, 261–280.
Jardetzky, O., Akasakan, K., Vogel, R., Morris, S., & Holmes, K. C. (1978) *Nature (London) 273*, 564–566.
Karplus, M., & McCammon, J. A. (1983) *Annu. Rev. Biochem. 53*, 263–300.
Klug, A. (1979) *Harvey Lect. 74*, 141–172.
Nelson, H. C. M., Hecht, M., & Sauer, R. T. (1983) *Cold Spring Harbor Symp. Quant. Biol. 47*, 441–449.
Pabo, C. O., & Lewis, M. (1982) *Nature (London) 298*, 443–447.
Pabo, C. O., Sauer, R. T., Sturtevant, J., & Ptashne, M. (1979) *Proc. Natl. Acad. Sci. U.S.A. 76*, 1608–1612.
Pabo, C. O., Krovatin, W. Jeffrey, A., & Sauer, R. T. (1982) *Nature (London) 298*, 441–443.
Perkins, S. J., & Dwek, R. A. (1980) *Biochemistry 19*, 245–258.
Piantine, V., Sorensen, O. W., & Ernst, R. R. (1982) *J. Am. Chem. Soc. 104*, 6800–6801.
Rance, M., Sorenson, O. W., Bodenhausen, G., Wagner, G., Ernst, R. R., & Wüthrich, K. (1983) *Biochem. Biophys. Res. Commun. 117*, 479–485.
Sauer, R. T., & Anderegg, R. (1978) *Biochemistry 17*, 1092–2200.
Sauer, R. T., Pabo, C. O., Meyer, B. J., Ptashne, M., & Backman, J. C. (1979) *Nature (London) 279*, 396–400.
States, D. J., Haberkorn, R., & Ruben, P. R. (1982) *J. Magn. Reson. 48*, 286–292.
Wade-Jardetzky, N., Bray, R. P., Onover, W. W., Jardetzky, O., Geisler, N., & Weber, K. (1979) *J. Mol. Biol. 128*, 259–264.
Weiss, M. A., Karplus, K., Patel, D. J., & Sauer, R. T. (1983) *J. Biomol. Struct. Dyn. 1*, 151–157.
Weiss, M. A., Eliason, J. L., & States, D. J. (1984) *Proc. Natl. Acad. Sci. U.S.A.* (in press).
Wüthrich, K., Wider, G., Wagner, G., & Braun, W. (1982) *J. Mol. Biol. 15*, 311–319.

Articles

Conformational Transitions of Thioredoxin in Guanidine Hydrochloride†

Robert F. Kelley and Earle Stellwagen*

ABSTRACT: Spectral and hydrodynamic measurements of thioredoxin from *Escherichia coli* indicate that the compact globular structure of the native protein is significantly unfolded in the presence of guanidine hydrochloride concentrations in excess of 3.3 M at neutral pH and 25 °C. This conformational transition having a midpoint at 2.5 M denaturant is quantitatively reversible and highly cooperative. Stopped-flow measurements of unfolding in 4 M denaturant, observed with tryptophan fluorescence as the spectral probe, reveal a single kinetic phase having a relaxation time of 7.1 ± 0.2 s. Refolding measurements in 2 M denaturant reveal three kinetic phases having relaxation times of 0.54 ± 0.23, 14 ± 6, and 500 ± 130 s, accounting for 12 ± 2%, 10 ± 1%, and 78 ± 3% of the observed change in tryptophan fluorescence. The dominant slowest phase is generated in the denatured state with a relaxation time of 42 s observed in 4 M denaturant. Both the slowest phase observed in refolding and the generation of the slowest phase in the denatured state have an activation enthalpy of 22 ± 1 kcal/mol. These features of the slowest phase are compatible with an obligatory peptide isomerization of proline-76 to its cis isomer prior to refolding.

The thioredoxin isolated from *Escherichia coli* contains 108 amino acid residues located in a single polypeptide chain having a single intrachain disulfide bond (Holmgren, 1968). Crystallographic analysis of the protein reveals it to contain a single twisted β-sheet composed of five strands flanked by four α-helical segments (Holmgren et al., 1975). These elements are integrated in a supersecondary structural array called the NAD binding domain, which has been observed to occur in a large number of proteins of diverse function. Since thioredoxin is the smallest monomeric protein known to contain an NAD binding domain, we consider it to be an excellent model protein for detailed studies of polypeptide chain folding. This paper describes equilibrium and kinetic measurements of the major conformational transition of *E. coli* thioredoxin using guanidine hydrochloride (Gdn-HCl)[1] as the denaturant at neutral pH. The majority of measurements were obtained with the protein having its single intrachain disulfide intact, a form we have denoted as oxidized thioredoxin. The principal novel observation is that the majority of the denatured protein refolds with a very long relaxation time, which likely results from the presence of a cis proline peptide bond in the native conformation.

Experimental Procedures

Materials. Thioredoxin was initially purified from *E. coli* B cells that were grown on minimal media and harvested at midlog phase by Grain Processing Corp. of Muscatine, IA. More recently the protein was purified from an *E. coli* strain constructed by Lunn et al. (1984) containing multiple copies of a plasmid with the gene for thioredoxin, which results in the cellular overproduction of thioredoxin by several hundred fold. Thioredoxin activity was measured by using the NADPH oxidation assay described by Laurent et al. (1964) and *E. coli*

† From the Department of Biochemistry, University of Iowa, Iowa City, Iowa 52242. *Received December 28, 1983.* This investigation was supported by U.S. Public Health Service Research Grant GM-22109 from the Institute of General Medical Sciences and by Program Project Grant HL-14388 from the National Heart, Lung and Blood Institute.

[1] Abbreviation: Gdn-HCl, guanidine hydrochloride.

0006-2960/84/0423-5095$01.50/0